

Downscaling of current and future rainfall climatologies for southern Morocco. Part I: Downscaling method and current climatology

H. Huebener^{a,*} and M. Kerschgens^b

^a *Institute for Meteorology, Freie Universität Berlin, Germany*

^b *Institute of Geophysics and Meteorology, University of Cologne, Germany, Carl-Heinrich-Becker-Weg 6-10, 12165 Berlin, Germany*

Abstract:

The use of a statistical-dynamical downscaling approach to obtain a high-resolution rainfall climatology for a subtropical region in southern Morocco is analysed. The statistical part of the downscaling uses Circulation Weather Types (CWTs) as a measure for near-surface wind fields calculated from sea-level pressure (SLP) data. The daily CWTs are correlated with daily rainfall data at three different climate stations in the region for the period 1978–1997 and systematic differences are discussed. Results are viewed for one extreme dry year (1984) and one extreme wet year (1989) to show the limits of purely statistical downscaling.

Dynamical downscaling is realized for representative days to enable statistical-dynamical downscaling. Comparison of statistically-dynamically downscaled rainfall with measured rainfall for the year 2002 and climatological results show that the method is capable of capturing the relevant mechanisms triggering rainfall in the area. For extreme dry (wet) years, rainfall is overestimated (underestimated) by the method and errors might occur even for normal years. However, application to a climatology calculated for the period 1958–1997 via analysing daily SLP fields from NCEP Reanalyses gives satisfactory results. For sufficiently long periods, the method is well capable of producing a reliable high-resolution rainfall climatology. We will therefore apply the method to climate change simulations in part II of this paper. Copyright © 2007 Royal Meteorological Society

KEY WORDS North Africa; precipitation; statistical-dynamical downscaling Circulation Weather Types

Received 4 August 2005; Revised 5 October 2006; Accepted 4 December 2006

INTRODUCTION

Semi-arid regions, such as southern Morocco, experience high interannual variability of scarce rainfall distribution and are most vulnerable to climatic changes. Average annual rainfall determines the production of biomass, thus affecting the capacity for farming, herding, and tourism (Le Houérou and Hoste, 1977; Parish and Funnell, 1999). Against this background, analysis of the regional impact of climate change on rainfall distribution is essential for planning and managing water demand and distribution in these regions.

Long-term data is mostly available in the form of General Circulation Model (GCM) simulations. These models have horizontal resolutions of hundreds of kilometers, and are therefore not suited to represent local effects properly. Additionally, the resolution is unsatisfactory for complex orographic terrain. In the case of North Africa, the high peaks of the Atlas Mountains (max. 4165m, Jebel Toubkal) cannot be resolved by GCMs. Nevertheless, the high Atlas Mountain ridge provides a significant

weather- and watershed for the region (Hasler, 1980; Nicholson and Kim, 1997). North of the Atlas Mountains, precipitation is often associated with depressions along the polar front. Several authors have successfully associated precipitation in the Mediterranean and northern Morocco with the phase of the North Atlantic Oscillation (NAO, e.g. Quadrelli *et al.*, 2001; Knippertz *et al.*, 2003a), while seasonal precipitation in spring is also at least partly influenced by the El Niño/Southern Oscillation (ENSO, e.g. Nicholson and Kim, 1997; Knippertz *et al.*, 2003c). However, the rain only seldom reaches the southern flank of the high Atlas. Rainfall there is more often associated with depressions off the Moroccan coast, steering moist air onto the African continent that might be released owing to forced lifting at the southern slopes of the Atlas Mountains. In several cases, moisture supply originates from tropical latitudes and is advected in the middle troposphere above the dry boundary layer northward along the western coast of Africa (Knippertz, 2003; Knippertz *et al.*, 2003b). Further east, the so-called Sharav cyclones play an increasingly important role in generating precipitation (Alpert and Ziv, 1989; Egger *et al.*, 1995). As the precipitation caused

*Correspondence to: H. Huebener, Institute for Meteorology, Freie Universität Berlin, Germany. E-mail: huebener@met.fu-berlin.de

by these processes is not well represented in GCMs, a reliable tool for downscaling meteorological information from GCM climate simulations is essential to determine the regional conditions (e.g. Trigo and Palutikof, 2001).

There are different approaches for downscaling meteorological information from GCMs to regional scales (see Yarnal *et al.*, 2001, for an overview). Statistical methods use known correlations of large-scale features that are well represented in GCMs to the variable to be investigated on the regional scale and apply these correlations to the GCM scenario output fields (e.g. Timbal, 2004; Zhao *et al.*, 2005). However, results obtained with this method are restricted with regard to the availability of measurements. Long-term measurements in the research area are scarce (if available at all) and it is only recently that some further stations have taken up measurements as part of the IMPETUS research project (An integrated approach to the efficient management of scarce water resources in West Africa). Thus, spatial information is not sufficient for a purely statistical downscaling approach. To add spatial information, dynamical simulations are used. The dynamical coupling of the downscaled information with the driving model enables spatial upscaling of the scarce measurements. It additionally allows application of the results to climate change simulations, as will be shown in the second part of this paper. Purely dynamical downscaling (e.g. Christensen *et al.*, 1997; Jones *et al.*, 1997; May and Roeckner, 2001) is computationally expensive and is therefore difficult to be applied to long periods of time, as is necessary to obtain climatological information.

Statistical-dynamical downscaling uses the advantages of both, the statistical approach and the dynamical approach. Large-scale fields with good correlations to the local effect to be investigated are statistically analysed to obtain relevant groups or classes of days for the meteorological field on the local scale that is in focus. Dynamical downscaling is then applied to representative days or episodes of the classes obtained. Finally, the dynamically simulated representatives of the classes are recombined according to the statistical distribution of the large-scale driving field. Statistical-dynamical downscaling has been successfully applied to rainfall and wind climatologies in different regions of the world (*cf* Fuentes and Heimann, 2000; Heimann, 2001). However, its use is limited by the availability of large-scale driving fields that contain sufficient correlation to the high-resolution field to be investigated.

Since the pressure fields are generally better represented in GCMs than precipitation distribution (e.g. Corte-Real *et al.*, 1995), patterns of sea-level pressure (SLP) or 500 hPa height are used frequently for downscaling purposes (e.g. Trigo and DaCamara, 2000; Trigo and Palutikof, 2001; Quadrelli *et al.*, 2001; Palutikof *et al.*, 2002). Circulation Weather Types (CWTs) calculated from daily SLP fields are known to have significant influence on dynamically induced rainfall for mid European regions (e.g. Buishand and Brandsma, 1997) or the Mediterranean (e.g. Palutikof *et al.*, 2002; Goodess and Palutikof, 1998). Several authors have shown that performance increases

when multiple fields are used for the classification. When aiming at precipitation, humidity fields are most beneficial (e.g. Enke *et al.*, 2005). However, in the region investigated here, a very dry boundary layer often prevents rainfall from reaching the ground, and humidity advection is often limited to relatively thin layers. Therefore, the simulation of humidity with a GCM is very difficult in this region. Since the analysis of a single field (SLP) yields good results, we decided to stick to this.

In this paper we will use objectively calculated CWT classifications (Jones *et al.*, 1993) to downscale rainfall in a subtropical region in North Africa. We selected this method for reasons of simplicity and easy extension to further data sets, since it uses a single variable that is available from reanalyses and GCM simulations in sufficient quality. CWTs have a sound physical basis and are easy to interpret as synoptic relevant patterns (Goodess and Palutikof, 1998). Furthermore, the results are surprisingly good, considering the possible errors due to presence of the Atlas Mountains in the analysis region. A meteorological model chain is employed for the dynamical downscaling. At the high-resolution end of this model chain, the non-hydrostatic prognostic mesoscale model FOOT3DK (**F**low **O**ver **O**rographically structured **T**errain, **3** **D**imensional, **K**öln Version) is used, which is nested in a one-way approach into the Lokal Model (LM) of the German Weather Service. Performance of the model chain and the FOOT3DK model is tested for the region and some necessary adjustments of soil moisture are implemented (Shao *et al.*, 2001; Hübener *et al.*, 2005).

In the section on Investigated Area and Data of this paper, we will give a short introduction to the investigated area and data used. In the section on Statistical Downscaling, the calculation of CWTs is described and the resulting climatological monthly CWT distribution for the National Centre for Environmental Prediction (NCEP) period (1958–1997) is shown. Thereafter, correlation of CWTs with rainfall at different climate stations will be discussed and the chosen station for further use in this study will be motivated. Results for the dry year (1984) and the wet year (1989) are presented to outline the reliability and also the limits of the purely statistical approach in the area. The section on Statistical-dynamical Downscaling briefly describes the model chain used for the dynamical downscaling and coupling of the statistical and dynamical methods. Results of the statistical-dynamical downscaling for the year 2002 are presented in the section on Results and compared with measured data in the area. Some additional remarks for the extreme years 1984 and 1989 are given. Finally, a climatology for the NCEP Reanalyses period (1958–1997) is presented. A short summary and suggestions for further research conclude the paper.

INVESTIGATED AREA AND DATA

The catchment of the Wadi Drâa is located at the southern slope of the high Atlas Mountains. In the valley

between the high Atlas and the anti Atlas lies the city of Ouarzazate (30°56'N, 6°54'W), where an artificial lake samples the waters from the parts lying above the catchment. From this reservoir, water is distributed into the irrigation channeling system down river. The simulation area covers the southernmost part of the catchment, where the river oasis comprises date palm groves fed by irrigation water. Further downstream, the river dries out and gives way to the Saharan desert (outlined in Figure 1, see Hubener *et al.*, 2005 for further information on the catchment). The research area has semi-arid climate, with less than 100 mm rainfall per year and potential annual evaporation rates of 2000 mm or more.

Daily rainfall data for the stations Ouarzazate (30°56'N, 6°54'W, WMO No. 60265), Er-Rachidia (31°56'N, 4°24'W, WMO No. 60210), and Bechar (31°37'N, 2°14'W, WMO No. 60571, see Figure 1 for location of the stations) is used to outline the physical soundness of CWTs as an approach to weather conditions in the region.

To test the reliability of downscaling results for the region, rainfall measurements for four climate stations are used: El Miyit (EMY, 30°21'50"N, 5°37'44"W), Asrir (ASR, 30°21'25"N, 5°50'10"W), Jebel H'ssain ou Brahmin (JHB, 29°56'12"N, 5°37'43"W), and Lac Ikriki (IRK, 29°58'23"N, 6°20'57"W) (triangles in Figures 1 and 6). The stations are part of the IMPETUS measurement network and started recording measurements between Dec 2000 (EMY) and Nov 2001 (IRK). Measurements are still continuing.

LM simulations to drive the nested high-resolution FOOT3DK simulations were only available for a 14 month period, from Nov 2001 to Dec 2002. Thus, the selection of representative days for the dynamical downscaling is restricted to this period. The problem will

be discussed in more detail in the section on Statistical-dynamical Downscaling.

To calculate CWTs, SLP data from the NCEP Reanalyses for the years 1958–1997 is used.

STATISTICAL DOWNSCALING

Calculation of CWTs

According to Jones *et al.* (1993), CWTs are calculated from SLP data at 16 points (asterisks in Figure 2(a)) distributed around the centre of the area of interest (here: 30°N, 5°W; black dots in Figure 2).

The calculation is based on the near-surface pressure gradient, assuming the near-surface wind field to be in first order parallel to the isobars. Thus, the following geostrophic wind and geostrophic vorticity definitions are used:

$$\vec{v}_g = \vec{i}u_g + \vec{j}v_g \tag{1}$$

$$u_g = -\frac{1}{\rho f} \frac{\partial p}{\partial y}, \quad v_g = \frac{1}{\rho f} \frac{\partial p}{\partial x} \tag{2}$$

$$\zeta_g = \frac{\partial v_g}{\partial x} - \frac{\partial u_g}{\partial y} \tag{3}$$

In Equations (1) to (3), \vec{v}_g is the geostrophic wind, with v_g and u_g the meridional and zonal components, and \vec{i} and \vec{j} the normal vectors in the zonal and meridional directions x and y . The air density and coriolis parameter are denoted ρ and f , respectively, and ζ_g is the geostrophic vorticity. Under the above mentioned assumption of first order geostrophic approximation near the surface, mean wind regimes are calculated for directional (Equations (4), (5), (6)) and rotational

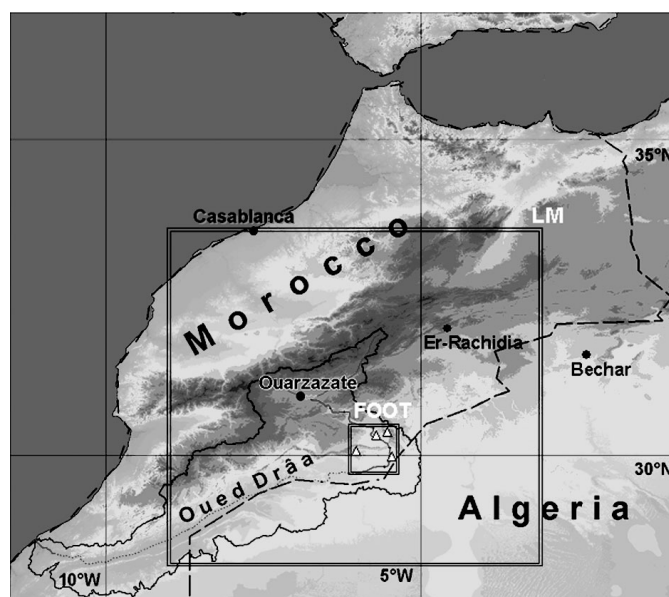


Figure 1. Wadi Draa (black outline), orography (colours), climate stations Ouarzazate, Er-Rachidia, and Bechar, simulation area of LM (large square) and of FOOT3DK (small square).

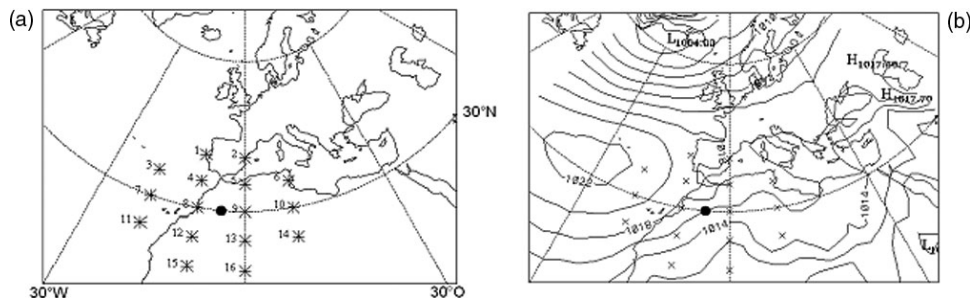


Figure 2. (a) Locations of the points where pressure values are used to calculate CWTs. (b) Mean climatological SLP field for NCEP reanalysis, 1958–1997. Isoline spacing is 2hPa.

(Equations (7), (8), (9)) components of the wind field.

$$W = \frac{1}{\sin(30^\circ)} \left(\frac{1}{2}(p_{12} + p_{13}) - \frac{1}{2}(p_4 + p_5) \right) \quad (4)$$

$$S = \frac{1}{\sin(30^\circ)} \left(\frac{1}{4}(p_5 + 2p_9 + p_{13}) - \frac{1}{4}(p_4 + 2p_8 + p_{12}) \right) \quad (5)$$

$$F = \sqrt{S^2 + W^2} \quad (6)$$

$$WV = \frac{1}{\sin(25^\circ)} \left(\frac{1}{2}(p_{15} + p_{16}) - \frac{1}{2}(p_8 + p_9) \right) - \frac{1}{\sin(35^\circ)} \left(\frac{1}{2}(p_8 + p_9) - \frac{1}{2}(p_1 + p_2) \right) \quad (7)$$

$$SV = \frac{1}{\sin(30^\circ)} \left[\left(\frac{1}{4}(p_6 + 2p_{10} + p_{14}) - \frac{1}{4}(p_5 + 2p_9 + p_{13}) \right) - \left(\frac{1}{4}(p_4 + 2p_8 + p_{12}) - \frac{1}{4}(p_3 + 2p_7 + p_{11}) \right) \right] \quad (8)$$

$$V = WV + SV \quad (9)$$

In Equations (4) to (9), p_i is the sea-level pressure at the position indicated by the index value (compare Figure 2(a)). The directional components consist of a westerly part W and a southerly part S . The total directional flow is given as F . Rotational flow consists of a westerly vorticity component WV and a southerly vorticity component SV , with total vorticity strength as their sum V . To account for different areas of representativeness due to the convergence of the meridians, trigonometric factors are added to the equations. Each daily SLP distribution is assigned to a directional class (if $|V| < F$), a rotational class (if $|V| \geq 2F$), a mixed class comprising a directional and a rotational class (if $F \leq |V| < 2F$), or a low wind situation (if $F < 4$ and $V < 4$).

Figure 2(b) shows the mean climatological SLP field for the NCEP Reanalyses for the years 1958–1997. Well-known features like Azores high and Island low are depicted as expected. Figure 3 shows the mean SLP

fields for composites over all days of every CWT in the left column, the middle column shows the anomaly of the composite CWT SLP fields from the climatological mean, and the right column depicts the standard deviation in each CWT. Particularly in the anomaly fields, meteorological interpretations of the CWTs come to mind. Extension of the Azores high towards southern Europe leads to north-easterly (NE) and easterly (E) flow at the southern flank of the high-pressure region. These CWTs are expected to be of little significance for rainfall, since the moisture must be advected from the Mediterranean, overflowing the Atlas Mountains east of the research area. South-easterly (SE), southerly (S), and south-westerly (SW) wind directions are diagnosed when a low-pressure anomaly at sea level is located off the Moroccan coast. At the southern flank of these systems (troughs or cut-off lows), moist air from the Atlantic Ocean can be advected onto the North African land mass. When this moist air reaches the southern slopes of the Atlas Mountains, rising motion is forced, leading to precipitation in the area. Westerly (W) CWT occurs when a negative SLP anomaly is located over the Iberian Peninsula. As for the SE, S, and SW CWTs, the westerly CWT might bring some precipitation south of the Atlas Mountains, when sufficiently moist air is advected from the Atlantic Ocean into the region. North-westerly (NW) and northerly (N) CWTs show a pressure distribution with low values over the western Mediterranean area, so the research area is located behind the trough. Therefore, owing to adiabatic sinking motion in the lee of the mountains, these CWTs are expected to account for mostly dry days even though lee cyclogenesis might occur infrequently, inducing the so-called Sharav cyclones (*cf* Alpert and Ziv, 1989; Egger *et al.*, 1995). Cyclonic (C) CWT is associated with a negative SLP anomaly centred over the research area. Since cyclonic motion is associated with rising air, these conditions favour rainfall if sufficient air moisture is available. During summer, however, cyclonic CWT often denotes heat lows over the Saharan desert region and is therefore not associated with rainfall. Anti-cyclonic (A) CWT shows positive sea-level pressure anomalies over the research area. Since this is associated with sinking motion, this CWT is expected to denote dry situations. However, some situations are classified as A, only because several small low-pressure spots are found around the centre of calculation in the SLP field. This

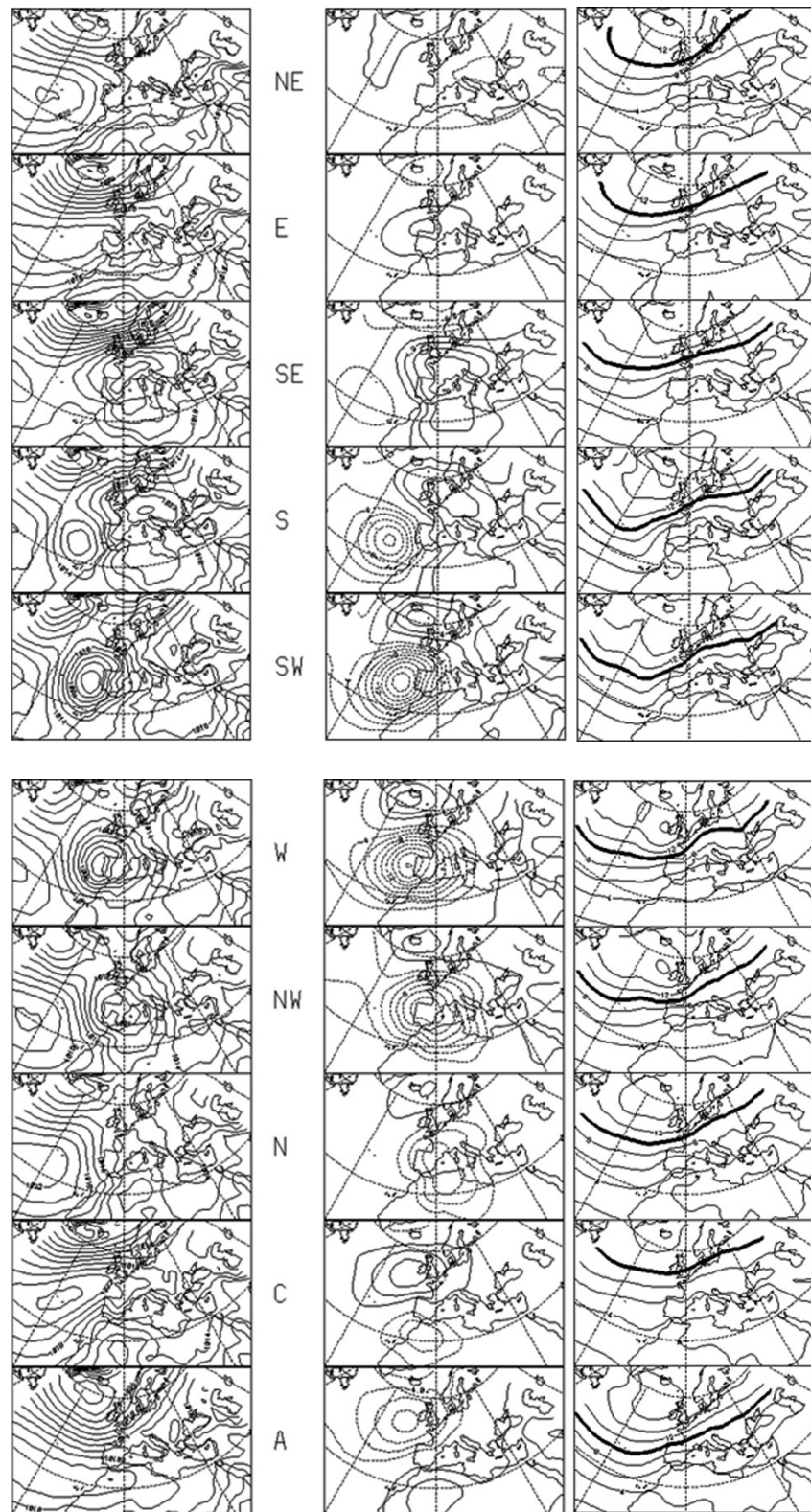


Figure 3. Pressure fields (left column), anomalies from mean field (middle column, dashed lines indicate negative anomalies), and standard deviation (right column) for each CWT. Isoline spacing is 2 hPa.

might explain the unusual rainfall occurrence on days with CWT A.

In-group variability (*cf* Enke *et al.*, 2005) in the CWTs is measured using the standard deviation (RMSE) from the composite of the respective CWT (Figure 3, right

column). It is found below 6 hPa in the direct research area but reaches values above 10 hPa (thick line) over the North Atlantic. However, the variability in the North Atlantic does not significantly influence the precipitation south of the high Atlas (Knippertz *et al.*, 2003b).

Table I. Correlation coefficients of station rainfall with CWTs for the whole year and winter (95% significant, light shaded; 99% significant, dark shaded).

	C	A	NE	E	SE	S	SW	W	NW	N
ORZ year	0.059	-0.081	-0.034	0.014	0.04	0.014	0.079	0.06	-0.005	-0.005
winter	0.187	-0.195	-0.054	-0.061	0.083	0.055	0.152	0.09	0.01	0.01
ERR year	0.081	-0.076	-0.012	-0.04	0.012	-0.003	0.01	0.015	0.026	0.049
winter	0.231	-0.167	-0.006	-0.042	0.023	-0.002	-0.051	0.037	0.044	0.021
BCH year	0.083	-0.074	0.001	-0.047	-0.019	-0.008	0.028	0.02	0.023	0.049
winter	0.202	-0.156	0.016	-0.075	-0.025	-0.024	0.046	0.041	0.089	0.103

Huebener and Kerschgens I Table I.

Climatology of CWTs and correlation to rainfall in the region

A climatology for the mean monthly distribution of CWTs for the area is presented in Figure 4(a) for the period 1958–1997. It shows an occurrence of the cyclonic class in all months of about 10% (grey). The anti-cyclonic class (green) is mainly confined to the winter months, while the NE (light yellow) and easterly (yellow) winds dominate the distribution during summer. SE (orange), southerly (red), SW (pink), and westerly (violet) winds rarely occur and are mostly restricted to the winter half year. North-westerly (blue) and northerly (cyan) winds are most frequent during spring, but can be found around the year, though only seldom.

Measured rainfall amount for stations Ouarzazate, Er-Rachidia, and Bechar (see Figure 1 for location of the stations) is distributed to the CWTs on the rainy days using the years 1978–1997. Results are presented in Figure 4(b–d) for Ouarzazate, Er-Rachidia, and Bechar. It should be noted that rainfall occurrence is associated with different CWTs for the three stations. While for Ouarzazate, the C (grey), SE (orange), S (red), and SW (pink) CWTs are the most relevant ones to produce rainfall (Figure 4(b)), this is not the case for Er-Rachidia (Figure 4(c)) and Bechar (Figure 4(d)). This is due to the precise locations of the stations (see Figure 1). The mean SLP field for all days with SE, S, and SW CWTs show negative pressure anomalies off the Moroccan coast, steering moist air from the Atlantic into the research area towards the southern slope of the Atlas Mountains (compare Figure 3). This mechanism becomes less efficient the further east the station is located. For Er-Rachidia and Bechar, precipitation is more often associated with N (cyan) and NW (blue) CWTs. Here, moisture can be advected from the Mediterranean. While the high Atlas mountain ridge effectively inhibits moisture advection in Ouarzazate due to adiabatic flow at the lee side of the

mountains, the height of the mountain ridge is less further east and moist air might pass into the African continent.

Correlation of CWTs with rainfall days is presented in Table I for all three stations for the whole year and restricted to the winter half year (October to March) for the period 1978–1997. Significant correlations are shaded (light: 95%, dark: 99%). All stations show significantly negative correlations of rainy days for anti-cyclonic CWT and significant positive correlations with cyclonic CWT. Further significant positive correlations are found for SW, westerly, and SE CWTs for Ouarzazate and for northerly and north-westerly CWTs for Bechar. For Ouarzazate, the high contribution of rainfall from the southerly CWT (Figure 4(b), red bars), associated with scarce occurrence (Figure 4(a), red bars) and not significant correlation with rainy days (Table I), implies particularly high rainfall amounts for events during this CWT. Correlations for all three stations tend to higher values when reduced to the winter half year, while they are lower during the summer half year (not shown).

Since the results for the three stations differ noticeably, we decided to use a single station, Ouarzazate, which is located nearest to the research area, to determine the relevant classes and their representatives to be simulated.

Results for an extreme dry and an extreme wet year

Monthly CWT distribution for the dry year (1984) and the wet year (1989) are displayed in Figure 5 (left hand side). In the dry year (1984) (Figure 5(a)), CWTs relevant for rainfall in the region (C, SW, S, SE, W) occur as often (9.62%) as in the climatological mean (9.63%, Figure 4(a)). Occurrence frequency of cyclonic CWT is particularly high in August (>20%), when this CWT is normally not associated with rainfall since it mostly depicts heat lows. In the wet year (1989), these CWTs are analysed noticeably more often (16.26%, Figure 5(c)). Therefore, analysis of annual occurrence

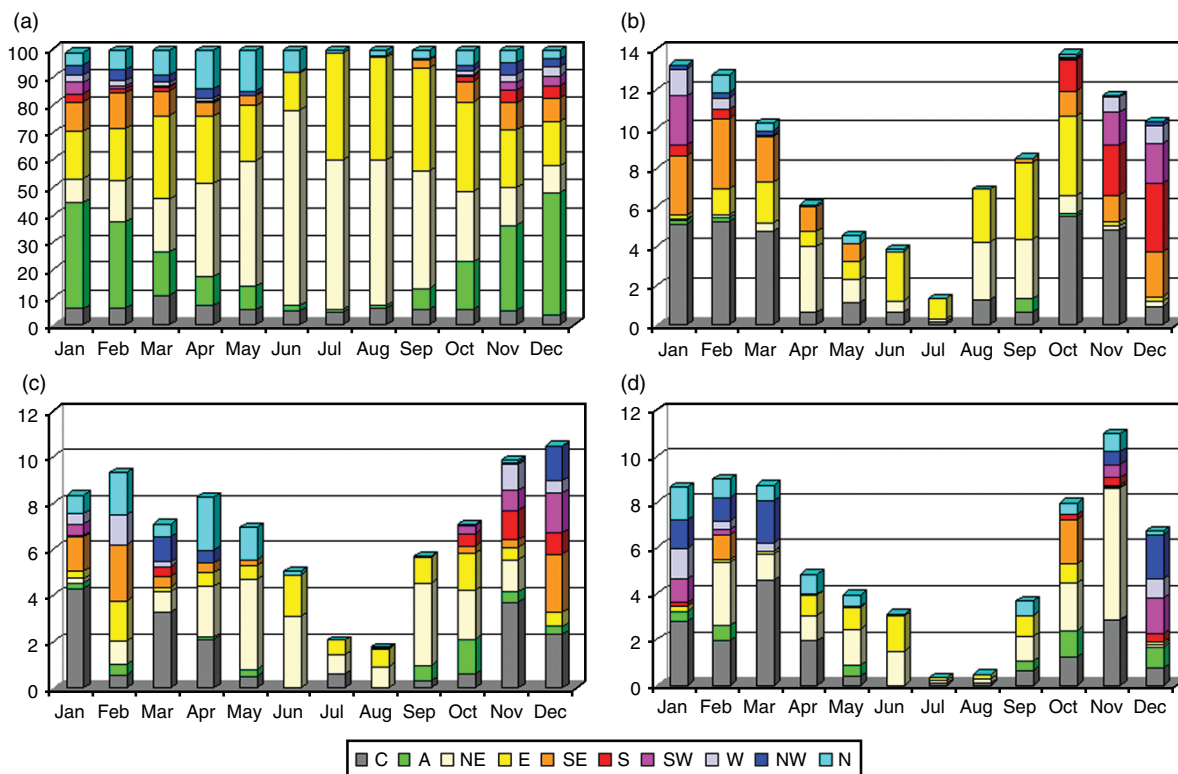


Figure 4. Climatological monthly CWT distribution (%) for NCEP reanalyses 1958–1997 (a). Mean monthly rainfall per CWT 1978–1997 for stations Ouarzazate (b), Er-Rachidia (c), and Bechar (d) in mm.

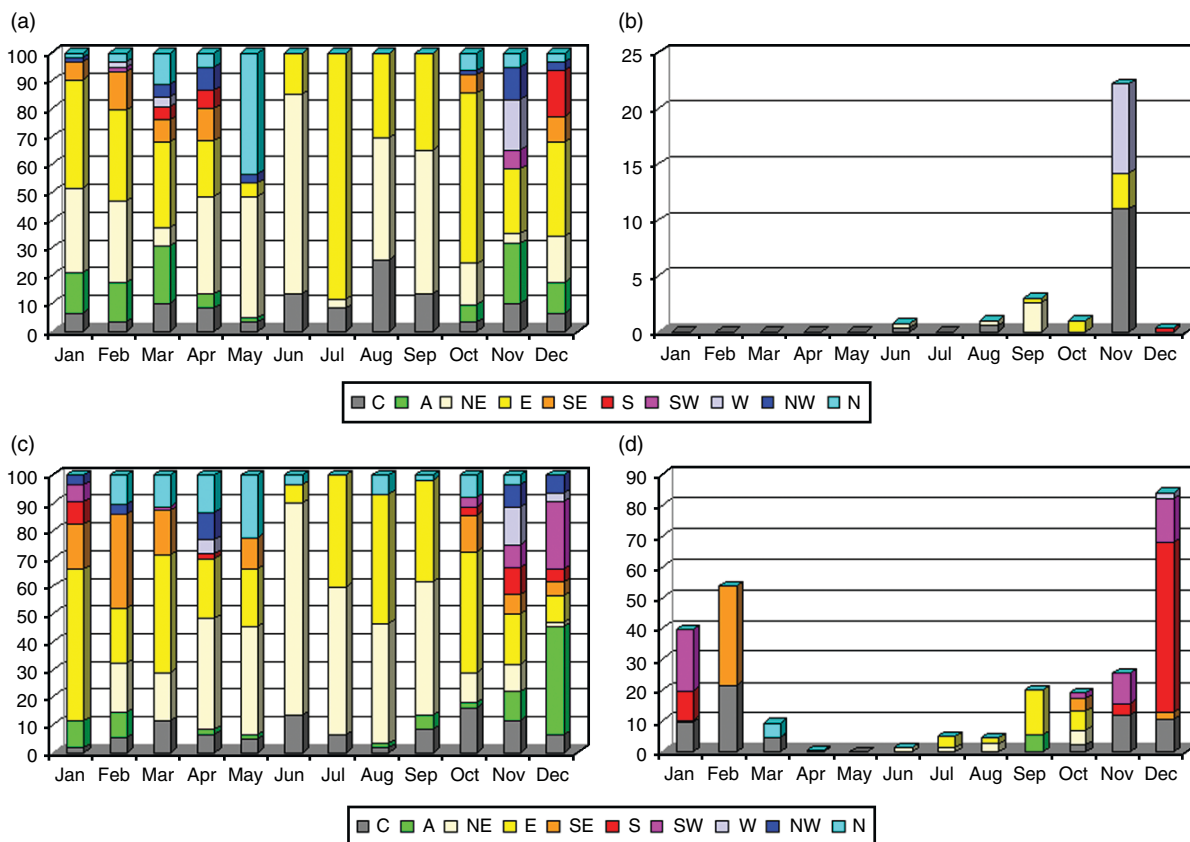


Figure 5. Monthly CWT distribution (left column, in %) and rainfall per CWT (right column in mm, note the different scaling) for the dry year 1984 (top) and the wet year 1989 (bottom).

frequency of CWTs might give a hint, but is not sufficient, to distinguish whether a year is exceptionally dry or wet or just normal.

Rainfall in 1984 (Figure 5(b)) consisted of two events on days with mixed CWTs (C + W, and C + E). In 1989, maximum precipitation occurred in January, February, and September to December, mostly in situations of troughs and their frontal systems off the Moroccan coast. In the periods 8–31 Aug 1989 and 14 Sept–5 Oct 1989, several events of tropical–extratropical interaction were observed (*cf.* Knippertz, 2003), which caused precipitation in the region.

STATISTICAL-DYNAMICAL DOWNSCALING

The model chain starts with analyses of the GME (global model of the German Weather Service, DWD). The regional model LM (Lokal Model of the DWD) is applied in two successive nesting steps (0.25° and $0.0625^\circ \approx 7$ km resolution) and driven with these analyses for the area depicted by the larger square in Figure 1 in the low resolution. Into the LM simulations, FOOT3DK is nested for the area indicated by the smaller square in Figure 1. FOOT3DK is a non-hydrostatic meteorological model. Horizontal resolution used in this work is $3 \text{ km} \times 3 \text{ km}$ for 40×40 grid boxes. In the vertical, a terrain following σ -coordinate is used and the resolution varies with height: 35 layers are distributed over a model height of 13 km, where the lowest layer has a thickness of 50 m and layer thickness increases with height. Implemented in FOOT3DK is a Soil-Vegetation-Atmosphere Transfer (SVAT) scheme, with two soil layers and one layer of vegetation. Implementation of a groundwater reservoir below the lower boundary of the model and irrigation is applied as described in Hubener *et al.* (2005). Further information on model physics and parameterizations can be found in Hubener *et al.* (2005) and Shao *et al.* (2001). A detailed discussion of simulation results and comparison to station measurements for a single day (2002/06/06) can also be found in Hubener *et al.* (2005).

The statistical-dynamical downscaling requires the separation of all days into disjunctive classes or groups and selection of representative days for each group. These representatives are dynamically simulated and thereafter statistically recombined to a synthetic climatology. Selection of appropriate days is restricted to the period when high-resolution LM simulations are available: November 2001 to December 2002. Station measurements in the research area are available from November 2001 to enable validation of the simulation results. Since in this region, as in most arid and semi-arid regions, rainfall typically consists of infrequent and often highly localized rainfall, it is difficult to select ‘typical’ rainfall events. Thus, to avoid dominating the results by a particular event, we selected two different days for each rainfall group to cover the in-group rainfall variability. As pointed out above, the year 2002 was neither an extreme dry nor an extreme wet year, and can be assumed to cover the typical range of rainfall events in the area.

Representatives for the CWT classes are obtained under the following conditions:

- LM simulations as nesting conditions were available for the period from November 2001 to December 2002. Representatives must therefore be selected from this period.
- To reduce the computing effort and avoid redundant information, CWTs are grouped according to their correlation with specific weather situations concerning rainfall as follows: (1) cyclonic; (2) anti-cyclonic; (3) NE and E; (4) SE, S and SW; (5) W; (6) NW and N.
- If possible, two days with rain and two days without rain are selected for each CWT-group. This is not possible in all cases. The LM period includes only one rainy day with CWT west and only one rainy day with CWTs north-west or north, and no rainy day with CWT anti-cyclonic. However, two simulations of anti-cyclonic days produce very small rainfall amounts in some grid boxes, so these days are taken as representatives for the anti-cyclonic group with rainfall. Westerly and north-westerly or northerly days with rainfall are represented by only one member.
- Representatives are restricted to pure directional or rotational days, no days with mixed classes are used.
- No low wind situations were allowed to serve as representatives.
- Actual representatives are subjectively selected from daily surface and 500 hPa maps from the European Weather Report (EWB), since an objective method (e.g. similarity to the composite field of the respective group) might not yield a typical day but a smoothed SLP distribution, particularly for groups associated with cyclones in the vicinity.
- Only those days are considered as rainy days where rainfall is measured at least at one of the stations in the research area and it is also simulated in the area (exception: anti-cyclonic group).
- If possible, the two representatives for each group are selected to account for the mean seasonal distribution of the group.

The days used as representatives are given in Table II. To obtain a climatology, weighting factors $W(R_i)$ are calculated for every representative day R_i in the following way:

$$W(R_i) = (\psi(C_i) \cdot \psi(P_i) / N(R_i(C_{iP})))$$

and

$$W(R_i) = (\psi(C_i) \cdot (100\% - \psi(P_i)) / N(R_i(C_{iOP})))$$

Where $\psi(C_i)$ is the occurrence frequency of the wind direction class (in %) of the representative R_i , $\psi(P_i)$ is the percentage of rainy days in this class. $N(R_i(C_{iP}))$ is the number of simulated representatives for this group

Table II. Representative days selected for the CWT classes with and without rainfall.

	C	A	NE, E	SE, S, SW	W	NW, N
With rain	2002/04/02	2001/12/07	2002/03/08	2001/12/10	2002/11/15	2002/05/22
	2002/05/06	2002/04/09	2002/08/28	2002/03/31		
Without rain	2002/02/17	2002/01/22	2001/12/04	2002/01/06	2002/04/08	2002/03/06
	2002/04/06	2002/03/10	2002/07/14	2002/10/28	2002/11/23	2002/12/28

Huebener and Kerschgens I Table II.

with rainfall, and $N(R_i(C_{ioP}))$ is the number of simulated representatives for this group without rainfall.

Since the selection of representative days for the CWT groups (in particular, of the rainy days) is crucial for the results, we will briefly address the question of rainy days in the CWT classes where rainfall is not readily expected. The two days representing the CWT A with rainfall show shallow pressure minima around the research area that are nevertheless associated with surface fronts. The days representing the E and NE CWT with rain both show a small scale wave disturbance in the SLP field that plausibly might favour rainfall in the research area. The day representing the NW and N CWT with rainfall is characterized by a strong front approaching the research area from NW and rain crossing the mountain ridge.

RESULTS

The results of the statistical-dynamical downscaling are compared to station measurements for the year 2002. Since the selected representatives are mostly taken from this year, the procedure should give reliable results for at least this year. Measurements at all four climate stations in the area were available for the whole year, thus the resulting rainfall distribution can be compared to measured rainfall at those stations.

Figure 6 shows the downscaled rainfall distribution for 2002 for the simulation region (coloured) and the measured values at the climate stations (triangles, coloured according to the same colour bar as the field values). The resulting rainfall distribution displays a noticeable rainfall gradient in the north–south direction. This seems to be in good agreement with reality, since the southern part of the research area is already part of the Saharan desert. In the northern part, precipitation is clearly bound to orographic barriers (isolines in Figure 6, compare also Figure 1 for orography). Simulated mean 2002 rainfall for the whole simulation area is 50.1 mm. Measured (simulated) rainfall at the stations is 45.2 (>120) mm for EMY, 64 (52.5) mm for ASR, 32.4 (52.5) mm for JHB, and 42.5 (30) mm for IRK. While local rainfall amounts for 2002 are well represented by the downscaling result for the stations ASR, JHB, and IRK, simulated rainfall is significantly overestimated, compared to measurements, at the station EMY. The maximum rainfall amount at the mountain ridge east of the station EMY must be regarded as too large. No station data was available to

validate the simulated rainfall maximum at the north-western border of the simulation area, but the values here should be regarded with caution, since this maximum is induced by inflow of moist air at the border of the model on a particular representative day. Keeping in mind the difficulties of comparing point measurements with simulated grid-box values for a 3 km × 3 km square, the results seem reasonable (barring the above-discussed problem).

Since the recombination for 2002 gives reliable results, in the following step the two extreme years, 1984 and 1989, are analysed to demonstrate the limits of the method. Since no measurements are available in the simulation domain for these years, results will be discussed in a general manner by comparison to rainfall at station Ouarzazate. Recombining the year 1984 with statistical-dynamical downscaling leads to an area mean annual rainfall of 21.7 mm for the simulation domain (not shown), which is as large as the precipitation in Ouarzazate for this year. Since rainfall in the simulation area typically amounts only to half the value at station Ouarzazate, this result is presumably an overestimation. Resulting downscaled precipitation for the wet year 1989 amounts to 92.8 mm (not shown), compared to 251.6 mm in Ouarzazate. This value seems underestimated, assuming that rainfall in the simulation area normally reaches half of the rainfall amount of Ouarzazate. We cannot prove the reliability of the method for the extreme years without ambiguity, since no measurements are available in the simulation area. However, we propose to desist from the method to simulate single years, since extreme events might be over- or underestimated. Nevertheless, it seems to be a reliable tool for climatological purposes, since smoothing of extreme values is required in this case.

A rainfall climatology is obtained for the NCEP Reanalysis period 1958–1997. The resulting distribution of precipitation is depicted in Figure 7. Mean rainfall is 31.9 mm for the whole area for the climatological year. The reduced area mean value is comparable to the 2002 simulation results from a smoother rainfall distribution and less prominent rainfall maxima, particularly at the mountainous region east of station EMY and in the north-western quarter of the simulation area. Since values for the 2002 simulation were expected to be overestimated in these locations, the reductions improve the overall picture.

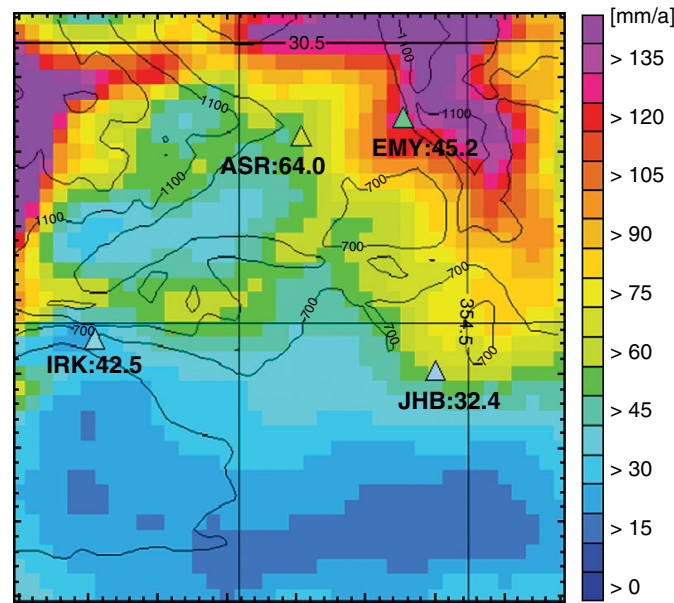


Figure 6. Rainfall distribution (mm/a) downscaled for 2002, triangles indicate measured rainfall for 2002 at IMPETUS stations.

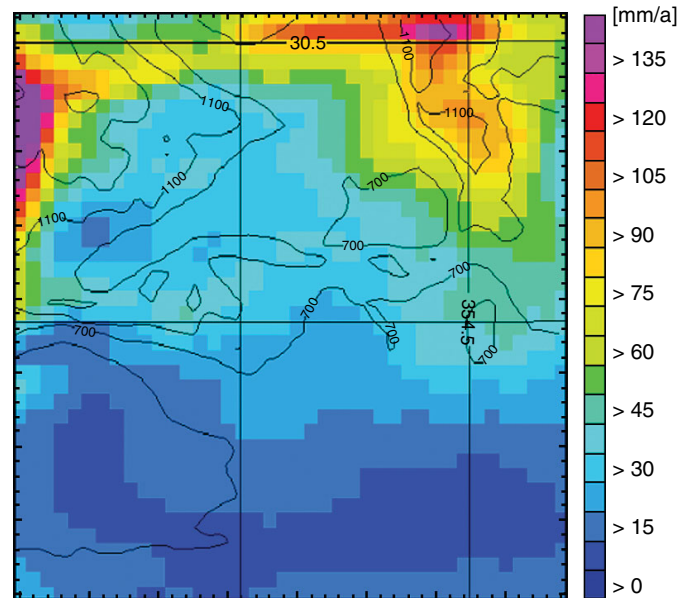


Figure 7. Climatological rainfall distribution (mm/a) for NCEP Reanalyses, 1958–1997.

SUMMARY

A method is developed not only to enable the analysis of current climate conditions at the northern border of the Sahara, but also to evaluate the impact of regional future climate change in the region. Since climate models usually feature coarse resolutions, and representation of local precipitation parameters (amount, seasonal distribution, extremes) is relatively poor, the adapted downscaling method uses SLP fields, which are better represented in climate models (e.g. Corte-Real *et al.*, 1995) and show good correlations with rainfall (e.g. Trigo and DaCamara, 2000; Trigo and Palutikof, 2001; Quadrelli *et al.*, 2001; Palutikof *et al.*, 2002; Knippertz *et al.*, 2003a). CWTs are objectively calculated according to Jones *et al.* (1993) for a region in southern Morocco located between the

high Atlas Mountains and the Saharan desert. Correlation of CWTs to precipitation at the stations Ouarzazate, Er-Rachidia, and Bechar shows that the method is able to capture a relevant part of rainfall-triggering conditions in the area. South of the Atlas Mountains, precipitation is highly correlated with negative SLP anomalies off the Moroccan coast. The results are in good agreement with previous findings by Knippertz *et al.* (2003a), who distinguished three different rainfall regimes in Morocco: the Atlantic coast north of the Atlas Mountains, the Mediterranean coast east of the Riff Mountains, and the Saharan border south of the Atlas Mountains. In addition to the results of Knippertz *et al.* (2003a), differences in physical relations of CWTs to rainfall mechanisms between three stations in the region south of the Atlas

mountains are clearly displayed in this work. While rainy conditions at stations in the western part of the region are correlated to southerly, SW, and SE winds, stations further east show enhanced rainfall contribution during northerly or north-westerly winds, as are typical for the formation of Sharav cyclones (Alpert and Ziv, 1989; Egger *et al.*, 1995).

The statistical analysis alone is not sufficient to give a detailed picture of rainfall distribution in a region with scarce measurements. Therefore, dynamically nested high-resolution simulations are realized, using a meteorological model chain consisting of global analyses of the German Weather Service (DWD), the regional model LM (Lokal Model of the DWD), and the mesoscale model FOOT3DK. Simulated representative days are recombined with respect to the statistical distribution of their respective CWT groups according to the statistical-dynamical downscaling procedure.

Comparison of statistical-dynamical downscaling results with measured precipitation for the year 2002 shows good agreement. However, applying the method to extreme dry (wet) years leads to overestimation (underestimation) of rainfall amounts, particularly in locations of higher rainfall in the simulation domain. As the region displays extreme interannual rainfall variability and the statistical-dynamical downscaling uses single days as representatives for a whole group of days, it should not be used for single years. It might be argued that the statistical-dynamical approach suffers from the smoothing of the extreme values and coarse temporal resolution, thus reducing the use of the high-resolution simulations. However, only high-resolution dynamical downscaling captures the rainfall patterns in orographically structured terrain correctly and allows the changes in the thermal and moisture fields to be taken into account when applying the method to climate change simulations.

Statistical-dynamical downscaling using CWTs as large-scale driving conditions gives a reliable picture of rainfall distribution for the NCEP climatology (1958–1997) in southern Morocco. We will therefore apply the method presented here to climate change simulations for this region in part II of this paper.

ACKNOWLEDGEMENT

The authors wish to thank the anonymous reviewer for helpful comments. They also wish to thank the DWD for providing the GME-Analyses and cpu-time for the LM runs. The authors particularly thank Dr K. Born, University of Cologne, for providing the LM simulations. This work was supported by the Federal German Ministry of Education and Research (BMBF) under grant No. 01 LW 0301A and by the Ministry of Science and Research (MWF) of the federal state of Northrhine-Westfalia under grant No. 223-21200200.

REFERENCES

- Alpert P, Ziv B. 1989. The Sharav cyclone: observations and some theoretical considerations. *Journal of Geophysical Research* **94**: D15, 18495–18514.
- Buishand TA, Brandsma T. 1997. Comparison of circulation classification schemes for predicting temperature and precipitation in the Netherlands. *International Journal of Climatology* **17**: 875–889.
- Christensen JH, Machenhauer B, Jones RG, Schär C, Ruti PM, Castro M, Visconti G. 1997. Validation of present-day regional climate simulations over Europe: LAM simulations with observed boundary conditions. *Climate Dynamics* **13**: 489–506.
- Corte-Real J, Zhang X, Wang X. 1995. Downscaling GCM information to regional scales: a non-parametric multivariate approach. *Climate Dynamics* **11**: 413–424.
- Egger J, Alpert P, Tafferner A, Ziv B. 1995. Numerical experiments on the genesis of Sharav cyclones: idealized simulations. *Tellus* **47 A**: 162–174.
- Enke W, Schneider F, Deutschländer T. 2005. A novel scheme to derive optimized circulation pattern classification for downscaling and forecast purposes. *Theoretical and Applied Climatology* **82**: 51–63, DOI: 10.1007/s00704-004-0116-x.
- Fuentes U, Heimann D. 2000. An improved statistical-dynamical downscaling scheme and its application to the Alpine precipitation climatology. *Theoretical and Applied Climatology* **65**: 119–135.
- Goodess CM, Palutikof JP. 1998. Development of a daily rainfall scenario for southeast Spain using a circulation-type approach to downscaling. *International Journal of Climatology* **10**: 1051–1083.
- Hasler M. 1980. *Der Einfluss des Atlasgebirges auf das Klima Nordwestafrikas*. Dissertation, Universität Bern. *Geographica Bernensia* **G11**: 171 S. (in German).
- Heimann D. 2001. A model-based wind climatology for the eastern Adriatic coast. *Meteorologische Zeitschrift* **10**: 5–16, DOI 10.1127/0941-2948/2001/0010-0005.
- Hübener H, Schmidt M, Sogalla M, Kerschgens M. 2005. Simulating evapotranspiration in a semi-arid environment. *Theoretical and Applied Climatology* **80**: 153–167, DOI 10.1007/s00704-004-0097-9.
- Jones PD, Hulme M, Briffa KR. 1993. A comparison of lamb circulation types with an objective classification scheme. *International Journal of Climatology* **13**: 655–663.
- Jones RG, Murphy JM, Noguer M, Keen AB. 1997. Simulation of climate change over Europe using a nested regional-climate model. Part II: comparison of driving and regional model responses to a doubling of carbon dioxide. *Quarterly Journal of the Royal Meteorological Society* **123**: 265–292.
- Knippertz P. 2003. Tropical-extratropical interactions causing precipitation in Northwest Africa: statistical analysis and seasonal variations. *Monthly Weather Review* **131**: 3069–3076.
- Knippertz P, Christoph M, Speth P. 2003a. Long-term precipitation variability in Morocco and the link to the large-scale circulation in recent and future climates. *Meteorological and Atmospheric Physics* **83**: 67–88, DOI 10.1007/s00703-002-0561-y.
- Knippertz P, Fink AH, Reiner A, Speth P. 2003b. Three late summer/early autumn cases of tropical-extratropical interactions causing precipitation in Northwest Africa. *Monthly Weather Review* **131**: 116–135.
- Knippertz P, Ulbrich U, Marques F, Corte-Real J. 2003c. Decadal changes in the link between El Niño and springtime North Atlantic oscillation and European-North African rainfall. *International Journal of Climatology* **23**: 1293–1311, DOI 10.1002/joc.944.
- Le Houérou HN, Hoste CH. 1977. Rangeland production and annual rainfall relations in the Mediterranean basin and in the African Sahelo-Sudan zone. *Journal of Range Management* **30**: 181–189.
- May W, Roeckner E. 2001. A time-slice experiment with the ECHAM4 AGCM at high resolution: the impact of horizontal resolution on an annual mean climate change. *Climate Dynamics* **17**: 407–420.
- Nicholson SE, Kim J. 1997. The relationship of the El Niño-Southern oscillation to African rainfall. *International Journal of Climatology* **17**: 117–135.
- Palutikof JP, Goodess CM, Watkins SJ, Holt T. 2002. Generating rainfall and temperature scenarios at multiple sites: examples from the Mediterranean. *Journal of Climate* **15**: 3529–3548.
- Parish R, Funnell DC. 1999. Climate change in mountain regions: some possible consequences in the Moroccan high atlas. *Global Environmental Change* **9**: 45–58.
- Quadrelli R, Pavan V, Molteni F. 2001. Wintertime variability of Mediterranean precipitation and its links with large-scale circulation anomalies. *Climate Dynamics* **17**: 457–466.

- Shao Y, Sogalla M, Kerschgens M, Brücher W. 2001. Effects of land surface heterogeneity upon surface fluxes and turbulent conditions. *Meteorology and Atmospheric Physics* **78**: 157–181.
- Timbal B. 2004. Southwest Australia past and future rainfall trends. *Climate Research* **26**: 233–249.
- Trigo RM, DaCamara CC. 2000. Circulation weather Types and their influence on the precipitation regime in Portugal. *International Journal of Climatology* **20**: 1559–1581.
- Trigo RM, Palutikof JP. 2001. Precipitation scenarios over Iberia: a comparison between direct GCM output and different downscaling techniques. *Journal of Climate* **14**: 4422–4446.
- Yarnal B, Comrie AC, Frakes B, Brown DP. 2001. Developments and prospects in synoptic climatology. *International Journal of Climatology* **21**: 1923–1950, DOI: 10.1002/joc.675.
- Zhao Y, Camberlin P, Richard Y. 2005. Validation of a coupled GCM and projection of summer rainfall change over South Africa, using a statistical downscaling method. *Climate Research* **28**: 109–122.